

# Ultra-Low Cross Polarization Microstrip Patch Antennas for Phased Arrays

José D. Díaz, *Student Member, IEEE*, Nafati Aboserwal, *Member, IEEE*, John T. Logan, *Member, IEEE*, Rick W. Kindt, *Member, IEEE*, Jorge L. Salazar, *Senior Member, IEEE*

**Abstract**—In this article, the authors present three microstrip patch antenna configurations for ultra low cross polarization phased arrays. These antennas are based on a mathematical model of an electric current in top of a dielectric covered ground plane. The model predicts that for linearly polarized antennas, -40 dB cross polarization can be achieved in the field of view of  $\theta = \pm 45^\circ$  and  $0^\circ \leq \phi \leq 180^\circ$ . To validate the model, HFSS planar electromagnetic simulations were made in where infinite ground plane and dielectrics are assumed. To extend the designs for planar phased arrays, an embedded element simulation using periodic boundary conditions was performed. Results show that microstrip antennas with -40 dB cross-polarization are possible by controlling effectively the dielectric characteristics under patch.

**Index Terms**—Low cross-polarization, microstrip patch antennas, phased array antennas.

## I. INTRODUCTION

IN the last couple of years, great attention have been directed to the design of low cross-polarization antenna elements for planar phased arrays, mostly driven by their need on weather radars [1], [2]. Since then, a plethora of antenna elements with low cross-polarization can be found in the literature with different bandwidths and scanning capabilities [3]–[7]. For dipole-like antennas [3], [4], an infinitesimal current over a ground plane has been used to estimate cross-polarization, while for microstrip patch antennas [5]–[7], the cavity model has shown good agreement with measurements [8]. These mathematical formulations can accurately predict the cross polarization for each type of antenna. However, they do not fully account for the characteristics of the dielectric which can play a large role in estimating cross polarization.

For example, for dipoles over a ground plane, the image current is invoked and the dielectric constant is assumed to be the same as air. This assumption, while reducing calculation complexity, fixes the cross polarization of a dipole to the order of -15 dB at  $\theta = 45^\circ$  and  $\phi = 45^\circ$ . For microstrip patch antennas, a similar argument can be made in where both, the height and the permittivity of the dielectric are omitted. When performed, the lowest achievable cross polarization in a microstrip patch antenna outside of the principal planes is about -25 dB. In this contribution, the authors make use of the electric current model [9] to calculate the electric field

J. Diaz, N. Aboserwal, and J. Salazar are with the Department of Electrical and Computer Engineering and the Advanced Radar Research Center (ARRC), The University of Oklahoma, Norman, OK, 73019. J. Logan and R. Kindt are with the Naval Research Laboratory (NRL), Washington, DC, 20375.

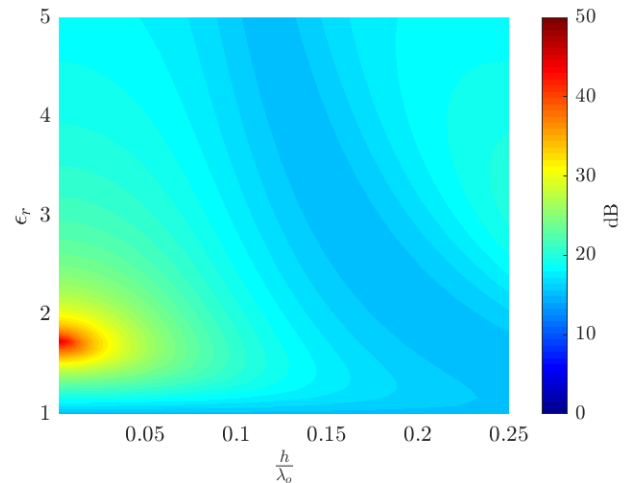


Fig. 1: Analytically derived maximum co- to cross-polarization at  $\theta = \pm 45^\circ$  and  $0^\circ \leq \phi \leq 180^\circ$  based on Ludwig's 3<sup>rd</sup> definition of polarization for a rectangular microstrip patch antenna element.

components  $E_\theta$  and  $E_\phi$  of microstrip antennas that includes the dielectric characteristics under the patch. Results show that for simple antenna structures, not only low profile but specific dielectric constants are necessary to achieve -40 dB cross-polarization in the scanning range of  $\theta = \pm 45^\circ$  and  $0^\circ \leq \phi \leq 180^\circ$ . With these results, the authors present three simple antenna design architectures applicable to ultra-low cross-polarization phased arrays.

## II. CROSS POLARIZATION PREDICTIONS BASED ON ELECTRIC CURRENT MODEL

To calculate the electric field components  $E_\theta$  and  $E_\phi$  for microstrip patch antennas, traditionally, antenna designers have used the cavity model. However, in its most basic form, the cavity model does not include the reflections from the dielectric covered ground plane [8]. In this contribution, we use a lesser known model called the electric current model [9], which is capable such fields and includes the characteristics of the dielectric. To properly use the electric current model, *a priori* knowledge of the antenna parameters is necessary. These parameters serve as inputs to the model and can be easily calculated with the relations shown in [8]. It is important to mention that the model assumes that only the dominant mode is propagating and no surface waves are excited. To

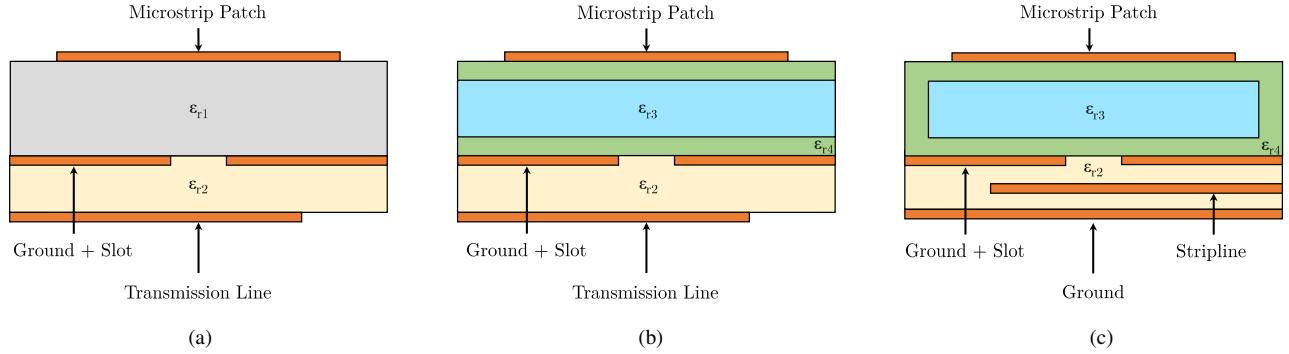


Fig. 2: Aperture coupled patch antennas stack-ups that can achieve -40 dB cross-polarization. (a) Transmission line fed aperture coupled patch antenna (b) Transmission line fed aperture coupled patch antenna with air gap. (c) Stripline-fed aperture coupled patch antenna with air-filled dielectric cavity. The permittivity for the dielectrics are as follows:  $\epsilon_{r1} = 1.6$ ,  $\epsilon_{r2} = 3.66$ ,  $\epsilon_{r3} = 1$ ,  $\epsilon_{r4} = 2.2$ .

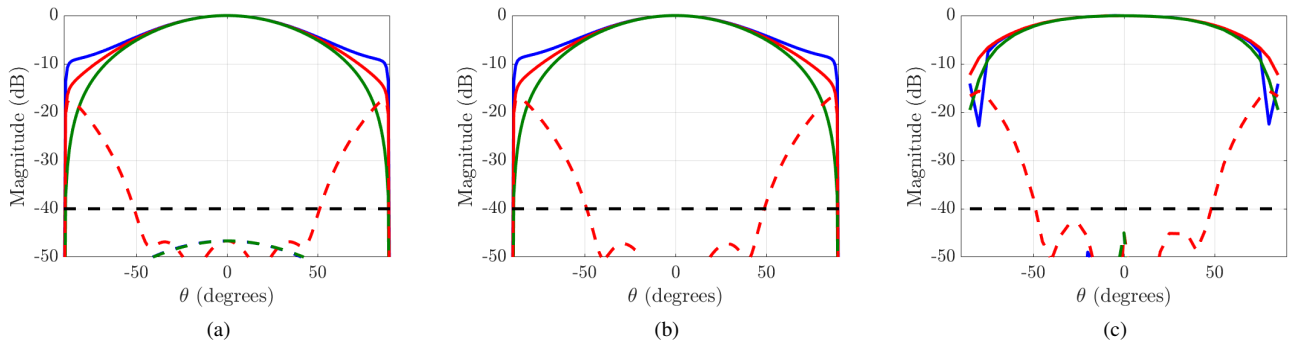


Fig. 3: Simulated radiation pattern for E-, D-, and H-planes. (a) Transmission line fed aperture coupled patch antenna (b) Transmission line fed aperture coupled patch antenna with air gap. (c) Stripline-fed aperture coupled patch antenna with air-filled dielectric cavity. Co-polarization (solid), cross-polarization (dashed), E-plane (blue), D-plane (red), H-plane (green).

calculate the cross polarization, Ludwig's 3<sup>rd</sup> definition of polarization is used for the case of an electrical current along the x-axis as shown in [10]. The relations for a rectangular patch antenna and the equations for the electric current model are all included in the Appendix A for clarity.

Using this knowledge, the maximum cross polarization in the field of view  $\theta = \pm 45^\circ$  and  $0^\circ \leq \phi \leq 180^\circ$  can be derived. Fig. 1 shows the maximum co- to cross-polarization difference for a rectangular microstrip antenna when the height and the permittivity of the dielectric are varied from  $0 \leq h \leq \lambda/4$  and  $1 \leq \epsilon_r \leq 5$ . It can be seen that for permittivity values close to 1.7 and profiles below  $0.025 \lambda$ , cross polarization levels below -40 dB can be achieved in the field of view of interest. Outside of this region, the cross polarization rapidly converges to values around -25 dB which is consistent with most of the microstrip patch antennas in the literature [5]. While simplified only in one figure, the model also tells the relation between bandwidth and cross polarization, which is: ultra-low cross polarization microstrip antennas on this configuration are inherently narrow band. This statement comes from the fact that to effectively increase the bandwidth in microstrip antennas, the height of the dielectric has to be increased.

### III. ULTRA-LOW CROSS-POLARIZATION PATCH ANTENNAS

Using the results from the previous section, three different microstrip patch antenna elements were designed to validate the mathematical model. Simulations were made using HFSS planar electromagnetics for the first two antennas in where infinite extension on ground planes and dielectrics is assumed. To excite the elements, the aperture coupled feeding technique was used. This technique avoids asymmetric radiation patterns that arise with the traditional probe feed [6]. Fig. 2a shows the stack-up of a linearly polarized antenna element fed by a  $50 \Omega$  transmission line. The square patch dielectric has a thickness of 40 mils with  $\epsilon_{r1} = 1.6$ , while the transmission line dielectric has a height of 30 mils and a  $\epsilon_{r2} = 3.66$ . The radiation pattern cuts for this antenna are shown in Fig. 3a. It can be seen that antenna is capable of achieving -40 dB cross polarization in the diagonal plane. However, when compared to the mathematical model, a slight discrepancy on the permittivity that achieves such cross polarization in Fig. 1 is evident (0.1 difference). This difference might be the result of the assumption that only the dominant mode is being excited in the model. Nevertheless, the results are evidence that exceptional control of the permittivity is required to achieve

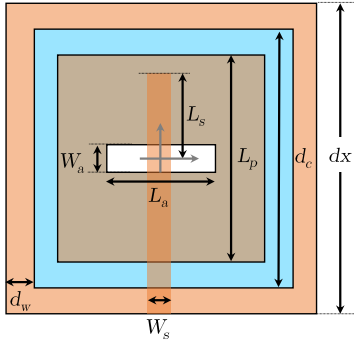


Fig. 4: Top-view of the stripline-fed aperture coupled patch antenna square unit cell simulated using periodic boundary conditions. The dimensions for the design were as follows:  $d_x = 50$  mm,  $d_c = 47$  mm,  $L_p = 34.76$  mm,  $L_a = 15.59$  mm,  $W_a = 2$  mm,  $W_s = 22$  mil,  $L_s = 13.1$  mm, and  $d_w = 1.5$  mm.

40 dB cross-polarization.

Moving on to a more practical design, Fig. 2b shows the second antenna stack-up in where only commercially available dielectrics are used. In this case, the patch dielectric is a combination of a 10 mil thick air gap ( $\epsilon_{r3} = 1$ ) and two dielectric cores with heights of 15 mil and  $\epsilon_{r4} = 2.2$ . The transmission line, again, has a characteristic impedance of  $50 \Omega$  on a 30 mil thick dielectric core with  $\epsilon_{r2} = 3.66$ . With this approach, the effective permittivity that the patch experiences is one that is somewhat averaged between the two dielectric cores and the air gap. Fig. 3b shows the radiation pattern cuts for this structure in where 40 dB cross polarization in the diagonal plane is again achieved. Notice, however, that both stack-ups (Fig. 3a and Fig. 3b) lack a backing ground plane which increases back radiation and makes the integration of the antenna with electronics more difficult. Also, neither of these configurations were embedded on periodic boundary conditions to account for the effects of mutual coupling if they were to be used for phased array applications. For these reasons, a stripline-fed microstrip patch antenna was designed.

Fig. 2c and Fig. 4 shows the third antenna stack-up and its top view when embedded on a square unit cell with length of  $d_x = 50$  mm. A square patch with dimensions of  $L_p = 34.76$  mm is above an air filled dielectric cavity. The cavity, which is also square, measures  $d_c = 47$  mm in extension and 15 mils in height. It is surrounded by a dielectric wall of  $\epsilon_{r4} = 2.2$  and thickness of  $d_w = 1.5$  mm. The dielectric cores above and below the cavity are 15 mil thick with  $\epsilon_{r4} = 2.2$ . The  $50 \Omega$  stripline has a width of  $W_s = 22$  mil and a stub length of  $L_s = 13.1$  mm. The aperture on the slotted ground has a width of  $W_a = 2$  mm and length of  $L_a = 15.59$  mm. While not added to the diagrams, vias between the ground and the slotted ground were placed around the periphery of the element to avoid any parallel plate modes. The radiation pattern cuts for the embedded element on the array and the active reflection coefficient are shown in Fig. 3c and Fig. 5.

It can be seen that -40 dB cross polarization was once again achieved in the diagonal plane. When comparing this element to the transmission line cavity approach shown in Fig. 2b, the

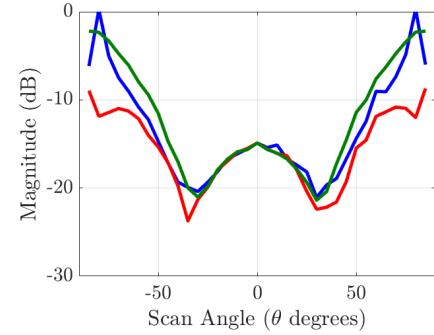


Fig. 5: Simulated active reflection coefficient for the stripline-fed aperture coupled patch antenna shown in Fig. 4. E-plane (blue), D-plane (red), H-plane (green).

cavity on the stripline case is 5 mil thicker. This difference might be attributed to the presence of the dielectric walls which are increasing the effective permittivity of the stack-up. When looking at the active reflection coefficient in Fig. 5, the reflections of the element are well below -10 dB in all planes up to  $50^\circ$ . It is not clear at this point whether or not the scan blindness that appears in the E-plane around  $\pm 85^\circ$  comes from the presence of the air-filled dielectric cavity. This will require further investigation.

#### IV. CONCLUSION

In this contribution the authors have shown three microstrip patch antenna elements with ultra-low cross-polarization. The elements are derived from the electric current model that predicts that not only the profile of microstrip antennas is important to achieve low cross-polarization but the dielectric permittivity under the patch. Results show that permittivity values around 1.7 and profiles around  $0.025\lambda$  are necessary to achieve cross-polarization of -40 dB in the field of view of  $\theta = \pm 45^\circ$  and  $0^\circ \leq \phi \leq 180^\circ$ .

#### APPENDIX A

##### ESTIMATING CROSS POLARIZATION

First, the input parameters of the antenna are calculated with the relations shown in [8]. The width of the patch can be calculated through,

$$W = \frac{c}{2f_o} \sqrt{\frac{2}{\epsilon_r + 1}},$$

in where  $c$  refers to the speed of light,  $f_o$  the operational frequency, and  $\epsilon_r$  the dielectric permittivity under the patch. Then, the effective permittivity of the dielectric,  $\epsilon_{reff}$ , is calculated to estimate the fringing fields extension using,

$$\epsilon_{reff} = \frac{\epsilon_r + 1}{2} + \frac{\epsilon_r - 1}{2} \left[ 1 + 12 \frac{h}{w} \right]^{-\frac{1}{2}},$$

in where  $h$  refers to the height of the dielectric. The fringing fields extensions can be calculated through,

$$\frac{\Delta L}{h} = 0.412 \frac{(\epsilon_{reff} + 0.3) \left( \frac{W}{h} + 0.264 \right)}{(\epsilon_{reff} - 0.258) \left( \frac{W}{h} + 0.8 \right)},$$

and the length of the patch by,

$$L = \frac{c}{2f\sqrt{\epsilon_{reff}}} - 2\Delta L \quad .$$

The next step to calculate the cross polarization is to use the previous variables as inputs to the electric current model to calculate  $E_\theta$  and  $E_\phi$ . The electric fields  $E_\theta$  and  $E_\phi$  are calculated by reciprocity through [9],

$$E_i(r, \theta, \phi) = E_i^{hex}(r, \theta, \phi) \left( \frac{\pi WL}{2} \right) \frac{\sin\left(\frac{k_y W}{2}\right) \cos\left(\frac{k_x L}{2}\right)}{\left(\frac{k_y W}{2}\right) \frac{\pi^2}{2} - \frac{k_x L}{2}},$$

in where the subscript  $i$  refer to either  $\theta$  or  $\phi$  electric fields. The superscript “hex” refers to the electric dipole or current sitting on top of the dielectric and  $k_x = k_o \sin \theta \cos \phi$  and  $k_y = k_o \sin \theta \sin \phi$ . The electric fields for the electric current along the x-axis are:

$$E_\phi^{hex}(r, \theta, \phi) = -E_o \sin \phi \cdot F(\theta) \quad ,$$

$$E_\theta^{hex}(r, \theta, \phi) = E_o \cos \phi \cdot G(\theta) \quad ,$$

in where  $F(\theta)$  and  $G(\theta)$  refer to the reflections from the ground given by,

$$F(\theta) = \frac{2 \tan(k_o h \sqrt{\epsilon_r - \sin^2 \theta})}{\tan(k_o h \sqrt{\epsilon_r - \sin^2 \theta}) - j \sqrt{\epsilon_r - \sin^2 \theta} \sec \theta} \quad ,$$

$$G(\theta) = \frac{2 \tan(k_o h \sqrt{\epsilon_r - \sin^2 \theta}) \cos \theta}{\tan(k_o h \sqrt{\epsilon_r - \sin^2 \theta}) - j \frac{\epsilon_r}{\sqrt{\epsilon_r - \sin^2 \theta}} \cos \theta} \quad .$$

The electric field magnitude  $E_o$  can be calculated through,

$$E_o = \left( \frac{-j\omega\mu_o}{4\pi r} \right) e^{-jk_o r} \quad ,$$

although only normalized results were shown throughout the paper. Finally, the co and the cross polarization for the x-polarized antenna are calculated with the relations,

$$u_{co} = E_\theta(r, \theta, \phi) \cos \phi - E_\phi(r, \theta, \phi) \sin \phi \quad ,$$

$$u_{co} = E_\theta(r, \theta, \phi) \sin \phi + E_\phi(r, \theta, \phi) \cos \phi \quad .$$

Fig. 6 and Fig. 7 serve as examples to see how important is the role of the permittivity under the patch to control the cross polarization.

## REFERENCES

- [1] D. S. Zrnic and R. J. Doviak, “System requirements for phased array weather radars,” in NOAA/NSSL, Tech. Rep., 2005.
- [2] Y. Wang and V. Chandrasekar, “Polarization isolation requirements for linear dual-polarization weather radar in simultaneous transmission mode of operation,” in IEEE Transactions on Geoscience and Remote Sensing, vol. 44, pp. 2019-2028, 2006
- [3] J. T. Logan, S. S. Holland, D. H. Schaubert, R. W. Kindt and M. N. Vouvakis, “A review of planar ultrawideband modular antenna (PUMA) arrays,” in 2013 International Symposium on Electromagnetic Theory, Hiroshima, 2013, pp. 868-871.
- [4] M. Mirmozafari, H. Saeidi-Manesh and G. Zhang, “Highly isolated crossed dipole antenna with matched copolar beams,” in Electronics Letters, vol. 54, no. 8, pp. 470-472, 19 4 2018.
- [5] J. A. Ortiz et al., “Ultra-compact universal polarization X-band unit cell for high-performance active phased array radar,” in 2016 IEEE International Symposium on Phased Array Systems and Technology (PAST), Waltham, MA, 2016, pp. 1-5.

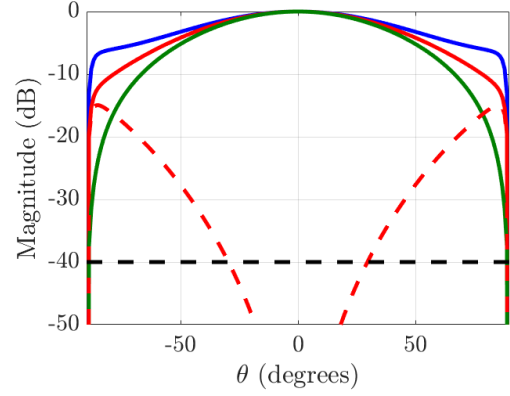


Fig. 6: Analytic patterns using the electric current model for a microstrip patch antenna with  $f_o = 3$  GHz,  $W = 39.5$  mm,  $L = 33.2$  mm, and  $\epsilon_r = 2.2$ , and  $h = 40$ mil. Co-polarization (solid), cross-polarization (dashed), E-plane (blue), D-plane (red), H-plane (green).

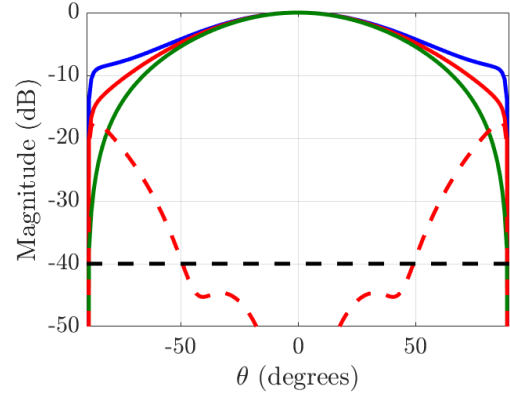


Fig. 7: Analytic patterns using the electric current model for a microstrip patch antenna with  $f_o = 3$  GHz,  $W = 42.7$  mm,  $L = 37.2$  mm, and  $\epsilon_r = 1.74$ , and  $h = 40$ mil. Co-polarization (solid), cross-polarization (dashed), E-plane (blue), D-plane (red), H-plane (green).

- [6] J. D. Diaz et al., “A cross-stacked radiating antenna with enhanced scanning performance for digital beamforming multifunction phased array radars,” in IEEE Transactions on Antennas and Propagation, vol. 66, no. 10, pp. 5258-5267, Oct. 2018.
- [7] H. Saeidi-Manesh and G. Zhang, “High-isolation, low cross-polarization, dual-polarization, hybrid feed microstrip patch array antenna for MPAR application,” in IEEE Transactions on Antennas and Propagation, vol. 66, no. 5, pp. 2326-2332, May 2018.
- [8] C. A. Balanis, Antenna theory: analysis and design. Wiley-Interscience, 2005.
- [9] D. R. Jackson and J. T. Williams, “A comparison of CAD models for radiation from rectangular patches,” in Intl. Journal of Microwave and Millimeter-Wave Computer Aided Design, vol. 1, no. 2, pp. 236-248, April 1991.
- [10] N. A. Aboserwal, J. L. Salazar, J. A. Ortiz, J. D. Diaz, C. Fulton and R. D. Palmer, “Source current polarization impact on the cross-polarization definition of practical antenna elements: theory and applications,” in IEEE Transactions on Antennas and Propagation, vol. 66, no. 9, pp. 4391-4406, Sept. 2018.